



Small asymmetric anthracene–thiophene compounds as organic thin-film transistors



Baji Shaik^a, Ji Hee Park^a, Tae Kyu An^b, Young Ri Noh^a, Soon Byung Yoon^a,
Chan Eon Park^b, Young Jin Yoon^a, Yun-Hi Kim^{a,*}, Sang-Gyeong Lee^{a,*}

^a Department of Chemistry, Research Institute of Natural Science (RINS), Graduate School for Molecular Materials and Nanochemistry, Gyeongsang National University, Jinju 660-701, Republic of Korea

^b Department of Chemical Engineering, Pohang University of Science and Technology, Pohang, 790-784, Republic of Korea

ARTICLE INFO

Article history:

Received 11 February 2013
Received in revised form 11 July 2013
Accepted 11 July 2013
Available online 18 July 2013

Keywords:

Organic thin-film transistors
Sonogashira coupling
Asymmetric anthracene derivatives
Solution processing
P-type charge carrier mobility

ABSTRACT

Anthracene and thiophene compounds are promising materials for OTFTs. We report here, the synthesis, as well as the physical, thermal, and optoelectronic properties of alkyl-substituted asymmetric anthracene–thiophene compounds connected by a bridged triple bond. The target molecules were synthesized using 2-bromoanthracene as the starting material, and the proceeding reactions included alkylation, bromination, and the Sonogashira coupling reaction. The synthesized compounds were both thermally and electrochemically stable. Among the synthesized compounds, **HTEA (7a)** and **DTEA (7b)** showed mobility and on/off ratio values of $1.3 \times 10^{-1} \text{ cm}^2/\text{V s}$, 2.6×10^6 and $2.0 \times 10^{-2} \text{ cm}^2/\text{V s}$, 1.0×10^6 , respectively.

© 2013 Elsevier Ltd. All rights reserved.

1. Introduction

Organic semiconductors came to light in the late 1940s. However, they still need to develop a lot compared to traditional inorganic semiconductors. With the first demonstration of organic semiconductors in the OLED field, OTFTs made a huge impact; this led to dramatic improvement in this research field. Organic semiconductors have many advantages over traditional inorganic semiconductors.^{1–7} Due to their ease of synthesis and low cost they have become of great interest in a short time. In recent years organic thin-film transistor research has become one of the major research areas. OTFTs have several applications in active matrix displays, RIF tags, and smart cards, etc.^{8,9}

The conjugation property of organic compounds is the key factor behind their semiconductor properties. During the last few years several organic compounds have been synthesized and used in OTFTs. Among them, thiophene, fluorene, anthracene, pentacene, carbazole, pyrene, naphthalene, and many other compounds and their derivatives have played a major role.^{10–20} Charge mobility is an important aspect in terms of OTFTs. Charge mobility depends on several factors such as the nature of the substance, process of device manufacturing, annealing process, and molecular packing. Among these, molecular packing is one of the most important parameters.

In the last few years, anthracene and thiophene compounds have been mostly synthesized for OTFTs. Most of the research has been done on polymers or symmetrical monomers or oligomers. Very few asymmetric compounds have been synthesized for the purpose of OTFTs;²¹ in contrast, more asymmetric molecules have been synthesized in other fields like pharmaceuticals. In the past, we synthesized asymmetric anthracene- and thiophene-based compounds connected by a double bond, and we found that they have the potential to be developed as OTFTs.²²

In this paper we report the synthesis of asymmetric anthracene–thiophene compounds connected by a triple bond. The thermal, physical, chemical, optical, and mobility properties have been extensively studied. We introduced alkyl chains to increase the solubility. In addition to the solubility, the end group alkyl chains have one more advantage in that they increase the molecular ordering, which enhances the charge mobility. The synthesized compounds **HTEA (7a)**, **DTEA (7b)**, **HBTEA (13a)**, and **DBTEA (13b)** are shown in Fig. 1. These compounds can be expected to give OTFT characters, even though the compounds are small and asymmetric.

2. Results and discussion

2.1. Optical properties

The optical properties of the synthesized compounds were investigated by using UV–visible absorption and photoluminescence

* Corresponding authors. Tel.: +82 55 772 1487; fax: +82 55 772 1489; e-mail address: leesang@gnu.ac.kr (S.-G. Lee).

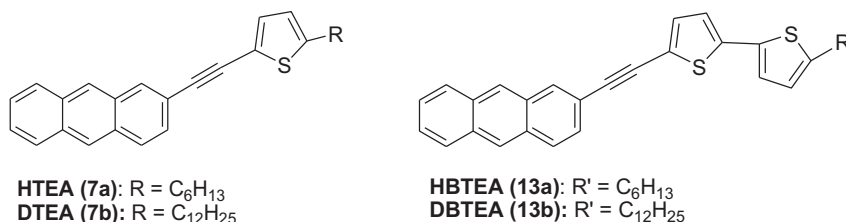


Fig. 1. Structure of HTEA (7a), DTEA (7b), HBTEA (13a), and DBTEA (13b).

(PL) spectra in a dilute CHCl₃ solution as well as on thin films. Figs. 2 and 3 represent the UV spectra and PL spectra, respectively, of the compounds. The films were made by dip-coating the materials on quartz in a chloroform solution at room temperature. The UV–vis absorption spectra of the four small molecules in thin films were red-shifted relative to those in solution. These phenomena can be explained by J-aggregation of the molecules,²³ which correlates with the particular molecular packing structure.²⁴ Intermolecular interactions between adjacent molecules in a solid state can be characterized by UV–visible spectroscopy. Based on the shift in the peak position, we can guess that the molecular packing structure in a film state of molecules. The red-shift in the UV absorption spectra can be interpreted as molecules stacked in a head-to-tail arrangement.²⁵ Therefore, the four synthesized molecules HTEA (7a), DTEA (7b), HBTEA (13a), and DBTEA (13b) were well arranged head-to-tail. These phenomena indicate that the small synthesized molecules can transfer electrons from one molecule to another easily. UV–visible absorption and PL emission spectral data are tabulated in Table 1. The HTEA (7a) and HBTEA (13a) films show a red-shift of 6 and 51 nm, respectively, in the UV region compared to the compounds in the dilute chloroform solution. This red-shift effect is as result of the formation of an aggregation or excimer in the thin film due to π – π^* stacking or intermolecular interaction caused by their planar structure leads to J-aggregations.²⁶

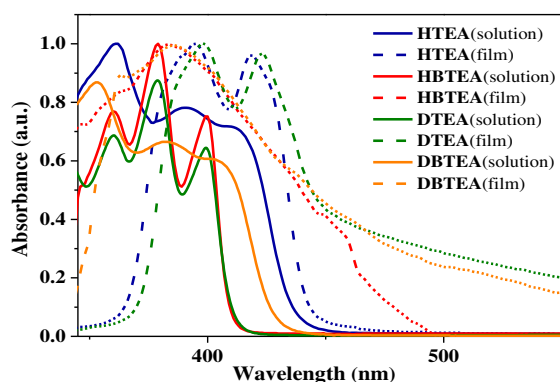


Fig. 2. UV–visible absorption spectra of HTEA (7a), DTEA (7b), HBTEA (13a), and DBTEA (13b) in a dilute CHCl₃ solution and thin film.

When compared to HTEA (7a) and DTEA (7b), the HBTEA (13a) and DBTEA (13b) films show a 12–30 nm high wavelength in the UV absorption spectrum due to an increase in conjugation attributed to the presence of one more thiophene ring. While in solution of HTEA (7a) has greater absorption value at 412 nm compared to the others due to the well-arranged structure of the hexyl side chain compared to the dodecyl side chain.

Based on their emission spectra, all the films show a clear, distinct red-shift of approximately 75–85 nm compared to the solution state. Among the four compounds DBTEA (13b) has a greater

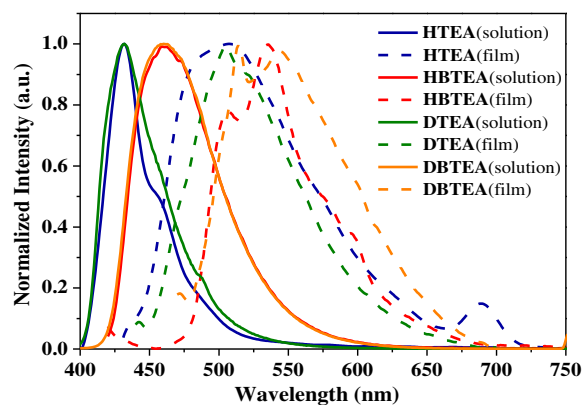


Fig. 3. Photoluminescence spectra of HTEA (7a), DTEA (7b), HBTEA (13a), and DBTEA (13b) in a dilute CHCl₃ solution and thin film.

Table 1
UV–visible and PL spectra of HTEA (7a), DTEA (7b), HBTEA (13a), and DBTEA (13b)

Compound	$\lambda_{\text{abs}}/\text{nm}^{\text{a}}$		$\lambda_{\text{em}}/\text{nm}^{\text{b}}$	
	Solution	Film	Solution	Film
HTEA (7a)	359, 391, 412	394, 418	430	508
DTEA (7b)	359, 378, 399	398, 422	431	504
HBTEA (13a)	361, 376, 398	383, 449	460	535
DBTEA (13b)	352, 382, 404	385, 436	461	545

^a Measured in a dilute CHCl₃ solution and thin-film state.

^b Excited at the absorption maxima.

absorption value at 545 nm while DTEA (7b) has the lowest absorption value at 504 nm. HBTEA (13a) and DBTEA (13b) have greater λ_{em} values than HTEA (7a) and DTEA (7b) both in the solution state and film state due to an increase in conjugation as a result of the introduction of one more thiophene ring.

2.2. Thermal properties

The thermal properties data of HTEA (7a), DTEA (7b), HBTEA (13a), and DBTEA (13b) revealed that all compounds were thermally stable. The TGA graphs of the four compounds are shown in Fig. 4. The decomposition temperatures with 5% weight loss for HTEA (7a), DTEA (7b), HBTEA (13a), and DBTEA (13b) were observed at 398 °C, 389 °C, 363 °C, and 410 °C, respectively. Among all the compounds DBTEA (13b) was the most thermally stable, while DTEA (7b) was the least thermally stable. The DSC graphs of the four compounds are shown in Fig. 5. The upper curve represents the first cooling while the lower curve represents the first heating. The endothermic melting point temperatures of HTEA (7a), DTEA (7b), HBTEA (13a), and DBTEA (13b) were observed at 128 °C, 103 °C, 195 °C, and 191 °C, respectively. The exothermic crystallization temperatures of HTEA (7a), DTEA (7b), HBTEA (13a), and DBTEA

(13b) were observed at 122 °C, 63 °C, 190 °C, and 190 °C, respectively. **HBTEA (13a)** and **DBTEA (13b)** have the highest crystallization temperature of 190 °C, while **DTEA (7b)** exhibited the lowest crystallization temperature of 63 °C. **HTEA (7a)** displays a high melting temperature and crystallization temperature compared to **DTEA (7b)**; in a similar way, this trend was also observed in **HBTEA (13a)** and **DBTEA (13b)**. Compounds containing the short alkyl side chain (hexyl) exhibited both a high melting temperature and crystallization temperature compared to compounds containing the long alkyl side chain (dodecyl). These data illustrate that all the compounds have a well-crystalline structure and can be used for making thin-film transistors.

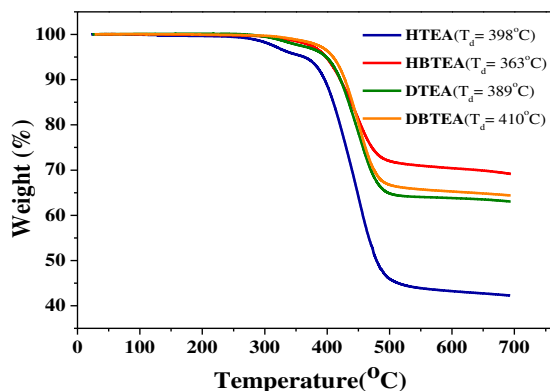


Fig. 4. TGA thermogram of **HTEA (7a)**, **DTEA (7b)**, **HBTEA (13a)**, and **DBTEA (13b)**.

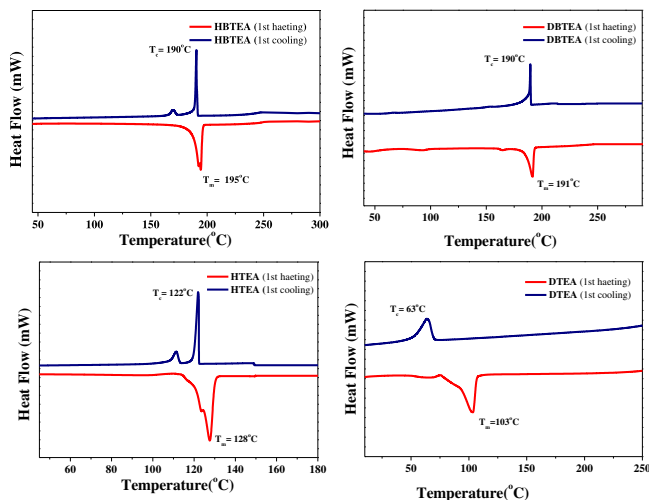


Fig. 5. Differential scanning calorimetry (DSC) thermogram of **HTEA (7a)**, **DTEA (7b)**, **HBTEA (13a)**, and **DBTEA (13b)**.

2.3. Electrochemical properties

Cyclic voltammetry (CV) measurements of the synthesized compounds were taken in order to determine the electrochemical stability, HOMO, and LUMO energy levels. CV graphs of the four compounds are shown in Fig. 6. The CV of **HTEA (7a)**, **DTEA (7b)**, **HBTEA (13a)**, and **DBTEA (13b)** was measured in a 1.0×10^{-3} M CHCl_3 solution containing 0.1 M Bu_4NClO_4 . The onset oxidation potential is summarized in Table 2. The onset oxidation potential E_{ox} values were 1.11, 1.17, 1.05, and 1.16 V for **HTEA (7a)**, **DTEA (7b)**,

HBTEA (13a), and **DBTEA (13b)**, respectively. **HBTEA (13a)** has the least oxidation potential compared to the others; this is due to the presence of the two thiophene rings, causing an increase in electron density in the compound, leading to it easily undergoing oxidation. **DTEA (7b)** was electrochemically more stable than the others and has a high onset oxidation potential, E_{ox} .

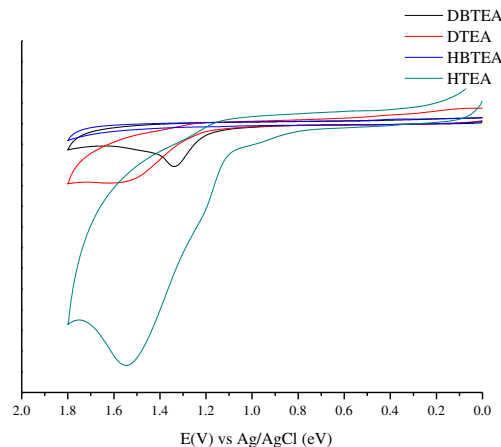


Fig. 6. Cyclic voltammogram of **HTEA (7a)**, **DTEA (7b)**, **HBTEA (13a)**, and **DBTEA (13b)** (working electrode: glassy carbon, reference electrode: Ag/AgCl in KCl (satd), counter electrode: Pt wire, electrolyte: 0.1 M TBAP in methylene chloride, purge time: 60 s, scan rate: 50 mV/s).

Table 2

Electrochemical properties of **HTEA (7a)**, **DTEA (7b)**, **HBTEA (13a)**, and **DBTEA (13b)**

Compound	Oxidation E_{onset} (V)	HOMO (eV)	LUMO (eV)	E_g (eV)
HTEA (7a)	1.11	-5.55	-2.72	2.73
DTEA (7b)	1.17	-5.61	-2.78	2.85
HBTEA (13a)	1.05	-5.49	-2.92	2.66
DBTEA (13b)	1.16	-5.60	-2.79	2.71

HOMO–LUMO gap measured according to the onset of UV absorption ($=1240/\lambda_{\text{onset}}$ eV), HOMO (eV) measured according to the onset of oxidation ($\text{HOMO} = 4.44 + E_{\text{onset}}$; ferrocene = $4.84 - E_{\text{onset}}$ (oxidation of ferrocene) = $4.84 - 0.40 = 4.44$).

These results suggest that these compounds have good electrochemical stability. The HOMO (LUMO) energy levels of **HTEA (7a)**, **DTEA (7b)**, **HBTEA (13a)**, and **DBTEA (13b)** were -5.55 (-2.72), -5.61 (-2.78), -5.49 (-2.92), and -5.60 (-2.79) eV, respectively. The LUMO energy level was calculated from the HOMO and E_g values. It was clearly observed that the HOMO–LUMO energy gap was less in both **HBTEA (13a)** and **DBTEA (13b)** than **HTEA (7a)** and **DTEA (7b)**; this is due to the increase in conjugation length, which lowers the HOMO–LUMO energy gap in both **HBTEA (13a)** and **DBTEA (13b)**.

2.4. XRD analysis

In order to determine the crystallinity and molecular packing XRD analysis was performed on the thin films of **HTEA (7a)** and **DTEA (7b)**. The XRD patterns of both films are shown in Fig. 7. Both **HTEA (7a)** and **DTEA (7b)** displayed diffractions through XRD analysis confirming their crystalline structure. **HTEA (7a)** showed its first strong reflection peak at $2\theta = 2.76^\circ$, with d-spacing 32.1 Å and the others are its second, third, and fourth orders, respectively. **DTEA (7b)** showed its first diffraction peak at $2\theta = 2.06^\circ$ with d-spacing 42.8 Å. From the XRD data, the π – π stacking ratio of the molecules in the in-plane phase showed that **HTEA (7a)** is exceptionally higher than **DTEA (7b)**. The more diffraction peaks in **HTEA**

(7a) compared to DTEA (7b) confirmed that, HTEA (7a) has more crystalline structure than DTEA (7b). And also, HTEA (7a) has well-ordered molecular crystals to compare with DTEA (7b). As a result of this, HTEA (7a) has higher charge mobility than the DTEA (7b).

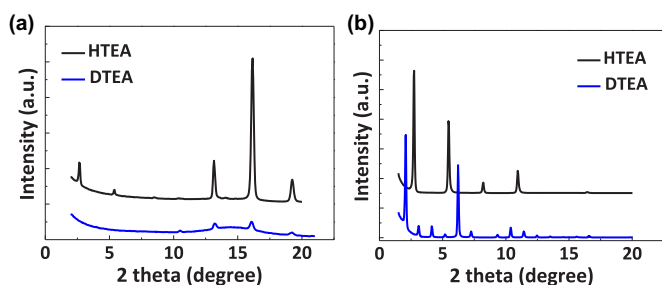


Fig. 7. XRD patterns of HTEA (7a) and DTEA (7b) [(a) in-plane (b) out-of-plane].

2.5. OTFT characterization

Top-contact OTFTs were made by depositing the drain and source electrodes above HTEA (7a) and DTEA (7b). The HTEA (7a) and DTEA (7b) layers were spin-coated from 0.7 to 0.5 wt % chloroform solutions, respectively. The mobility, on–off ratio, and threshold voltage of the films of HTEA (7a) and DTEA (7b) are tabulated in Table 3. The voltage–current graphs are represented in Figs. 8 and 9. Figs. 8a and 9a show plots of the drain current (I_D) versus gate voltage (V_G), and Figs. 8b and 9b show plots of the drain current (I_D) versus drain-source voltage (V_D) for HTEA (7a) and DTEA (7b)-based OTFTs. From the graphs it was clearly evident that when the gate voltage decreased to below zero, there was a sudden increase in drain current flow, indicating P-type OTFTs. The current increases linearly with drain voltage, at low drain voltages. When the drain voltage reaches to the gate voltage, the voltage drop at the drain contact falls to zero, and the conducting channel is pinched off, this is known as saturated regime. At this stage current becomes independent of the drain voltage. In the saturated regime, $V_D \geq (V_G - V_T)$. Field-effect mobility was calculated in the saturation regime using the equation $I_D = (W/2L)\mu C_i (V_G - V_T)^2$. Where I_D is the source-drain current, V_D is the source-drain voltage, V_G is the gate voltage, V_T is the threshold voltage, and C_i is the capacitance per unit area of SiO₂ layer. The HTEA (7a)-based OTFT showed a higher performance in terms of both mobility (1.3×10^{-1} cm²/V s) and on/off ratio (2.6×10^6), due to HTEA (7a) having a more crystalline structure than DTEA (7b). XRD data confirmed the more crystalline structure of HTEA (7a) compared to DTEA (7b). In addition, the short alkyl side chain in HTEA (7a) favored the well-ordering of molecules. This crystalline structure and the well-ordered molecular arrangement in HTEA (7a) lead to easy charge transport. As a result, HTEA (7a) exhibited high mobility compared to DTEA (7b). DTEA (7b) exhibited a mobility of 2.0×10^{-2} cm²/V s and an on/off ratio of 1.0×10^6 . The greater solubility of HTEA (7a) and DTEA (7b) enabled the production of OTFTs. On the other hand, the low solubility of HBTEA (13a) and DBTEA (13b) disfavored the making of OTFTs.

Table 3
TFT properties of HTEA (7a) and DTEA (7b)

	Mobility (cm ² /V s)	On/off ratio	Threshold voltage (V)
HTEA (7a) ^a	1.3×10^{-1}	2.6×10^6	−1.43
DTEA (7b) ^b	2.0×10^{-2}	1.0×10^6	−5

^a Top-contact, OTS, spin-coating (chloroform 0.7 wt %, 4000 rpm, 60 s).

^b Top-contact, OTS, spin-coating (chloroform 0.5 wt %, 2000 rpm, 60 s).

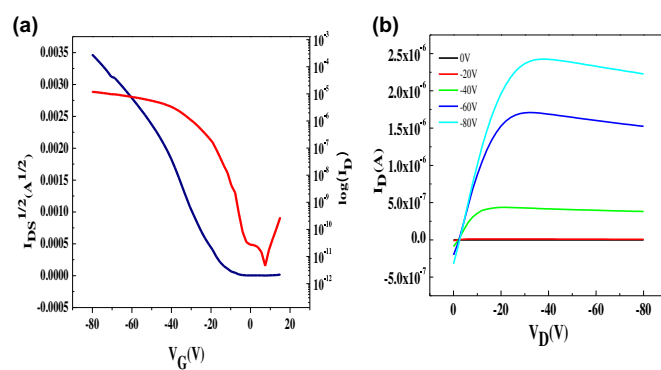


Fig. 8. (a) Drain current (I_D) versus gate voltage (V_G) characteristics of HTEA (7a). (b) Drain current (I_D) versus drain-source voltage (V_D) characteristics of the HTEA (7a) OTFT at different gate voltages (V_G).

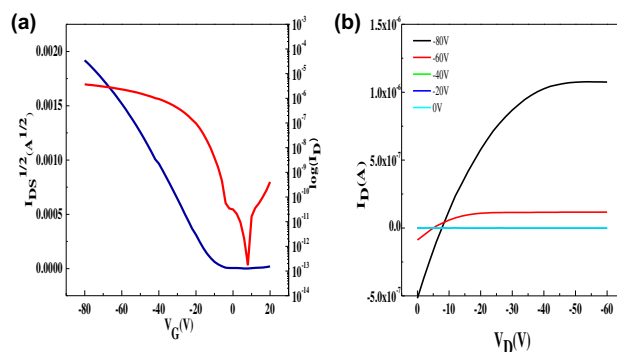


Fig. 9. (a) Drain current (I_D) versus gate voltage (V_G) characteristics of DTEA (7b). (b) Drain current (I_D) versus drain-source voltage (V_D) characteristics of DTEA (7b) OTFT at different gate voltages (V_G).

3. Conclusions

In conclusion, we synthesized asymmetric HTEA (7a), DTEA (7b), HBTEA (13a), and DBTEA (13b) by using the Sonogashira coupling reaction and other reactions, and examined their optical, thermal, and electrochemical properties. Examination of their thermal properties revealed that the four materials have good thermal stability. Investigation of their optical and electrochemical properties revealed that DTEA (7b) and DBTEA (13b) had higher oxidation potentials due to their higher HOMO energy levels [−5.61 eV for DTEA (7b), −5.60 eV for DBTEA (13b)]. HTEA (7a) and DTEA (7b) showed good solubility in toluene and chlorobenzene, and were also soluble in chloroform after heating. HBTEA (13a) and DBTEA (13b) showed good solubility in toluene and chlorobenzene under hot conditions, but were sparingly soluble in chloroform under both cold and hot conditions. The greater solubility of HTEA (7a) and DTEA (7b) enabled OTFTs to be made. Devices using HTEA (7a) and DTEA (7b) thin films were prepared by spin-coating, and exhibited a mobility of 1.3×10^{-1} cm²/V s with an on/off current ratio of up to 2.6×10^6 and a threshold voltage of −1.43 V, [HTEA (7a)]; a mobility of 2.0×10^{-2} cm²/V s, on/off ratio of 1.0×10^6 and threshold voltage of −5 V [DTEA(7b)]. These results suggest that the presence of a short alkyl side chain leads to a well-ordered molecular arrangement and shows good mobility. We hope this research will enhance the development of more asymmetric compounds in the field of OTFTs as well as in the field of organic semiconductors.

4. Experimental section

4.1. General methods

4.1.1. Materials. All the reagents and chemicals were purchased from Sigma–Aldrich Co. The solvents such as tetrahydrofuran

(THF), diethyl ether, toluene, and acetonitrile were used after distillation in the presence of sodium/benzophenone or calcium hydride under nitrogen gas. Chromatography was performed on silica gel (70–230 mesh, Merck) using gravity flow.

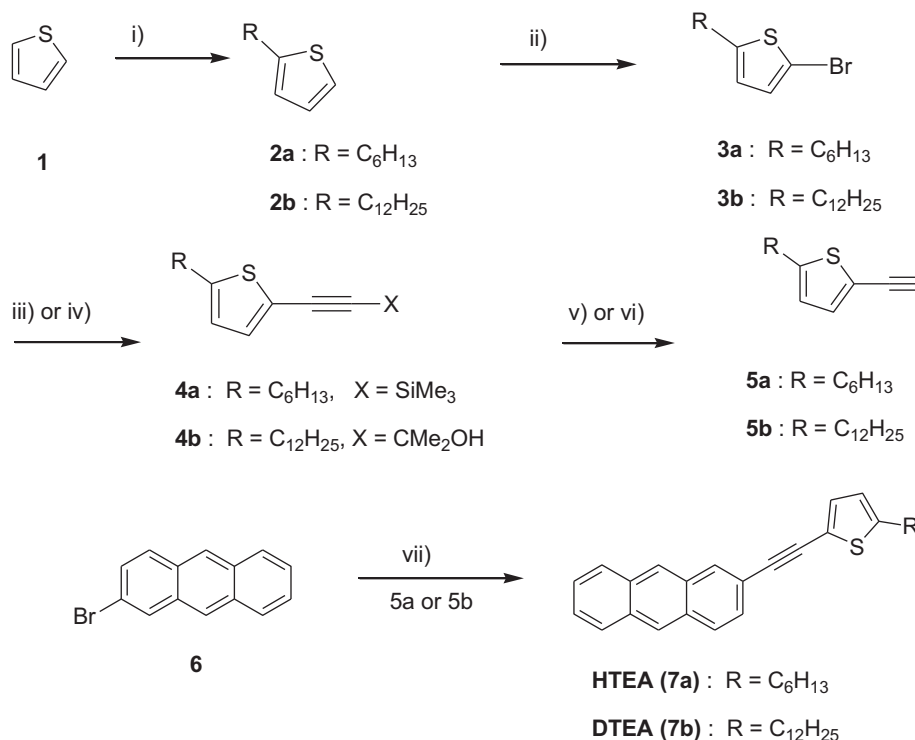
4.1.2. Spectroscopic measurements. ^1H and ^{13}C NMR spectra were recorded on 300 MHz and 75 MHz spectrometers, respectively. The chemical shift values were reported in δ units (ppm) relative to an internal standard (TMS). Mattson genesis series FTIR spectrophotometer was used for IR analysis. Mass spectra analysis was carried on a JMS-700, JEOL. UV–visible absorption and photoluminescence (PL) spectra were obtained by using Perkin–Elmer LAMBDA-900 UV/VIS/NIR spectrophotometer and an LS-50B luminescence spectrophotometer, respectively. The XRD data was obtained from mode X-ray diffraction (1D XRD) spectroscopy at the 5 Å beam line in the Pohang Accelerator Laboratory.

4.1.3. Electrochemical measurements. Cyclic voltammogram measurements were carried out on an epsilon E_3 at room temperature in a tetrabutylammonium perchlorate (0.1 M solution) in acetonitrile under nitrogen atmosphere at a scan rate of 50 mV/s. A Pt wire and Ag/AgCl electrodes were served as the counter and reference

silicon as gate with a thickness of 300 nm, thermally grown on SiO_2 dielectric layer. The octadecyltrichlorosilane monolayer was treated in toluene solution for about 2 h. Solutions of the organic semiconductors were spin-coated at 4000 rpm from 0.7 wt %, 4000 rpm from 0.7 wt % chloroform solutions to get **HTEA** and **DTEA** thin films, respectively. Gold source and drain electrodes were evaporated on top of organic layers (100 nm). The channel length and width were 100 μm and of 2000 μm , respectively. The electrical measurements of the OTFETs were obtained in an air with the help of KEITHLEY 2400 and 236 source/measure units. Field-effect mobilities were measured in the saturation regime, by using the slope of the source-drain graph.

4.2. Synthesis

The asymmetric **HTEA** (**7a**), **DTEA** (**7b**), **HBTEA** (**13a**), and **DBTEA** (**13b**) were synthesized according to Schemes 1 and 2. Compounds **6** and **8** were synthesized according to literature procedure and the spectral data were coincided with literature data.^{27,28}

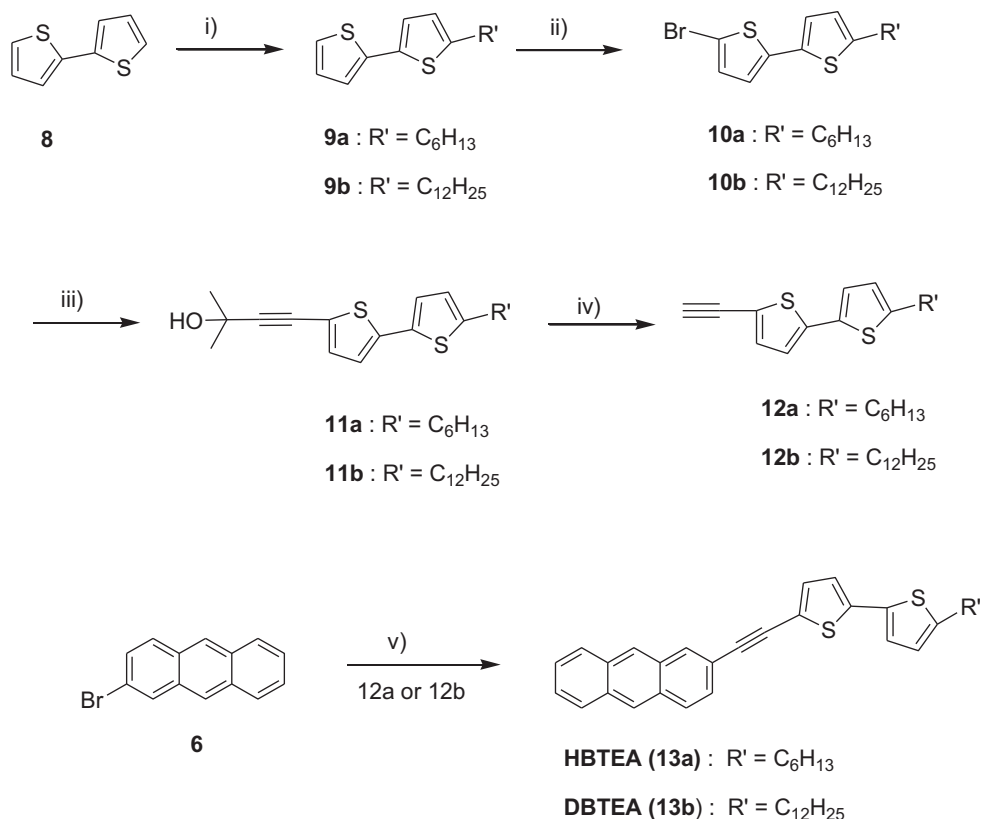


Scheme 1. Synthesis of **HTEA** (**7a**) and **DTEA** (**7b**). Reagents and conditions. (i) *n*-BuLi, 1-bromohexane; (ii) NBS, AcOH, chloroform; (iii) ethynyltrimethylsilane, Pd(*p*ph₃)₂Cl₂, CuI, *i*-Pr₂NH, reflux; (iv) 2-methyl-3-butyne-2-ol, Pd(*p*ph₃)₂Cl₂, CuI, Et₃N, reflux; (v) Bu₄NF, THF; (vi) KOH, *i*-PrOH, reflux; (vii) Pd(*dppf*)₂Cl₂, CuI, toluene, *i*-Pr₂NH.

electrodes, respectively. Melting points were measured with the electrothermal Mode 1307 digital analyzer and were uncorrected. Differential scanning calorimetry (DSC) measurements were carried out under nitrogen by using a TA instruments 2100 differential scanning calorimeter, by heating from 30 °C to 300 °C at a rate of 10 °C/min. Thermogravimetric analysis (TGA) was obtained under nitrogen by using a TA instruments 2050 thermogravimetric analyzer, by heating at a 10 °C/min heating rate from 30 °C to 700 °C.

4.1.4. Device fabrication and characterization of field-effect transistors. Top-contact OTFETs were fabricated on highly n-doped

4.2.1. 2-Hexylthiophene (2a). To a solution of thiophene (5.0 g, 60 mmol) in THF (50 mL) was added dropwise *n*-BuLi (40.6 mL, 65 mmol, 1.6 M in hexane) at –78 °C. The reaction mixture was stirred for 1 h at –78 °C under nitrogen. To the reaction mixture added slowly 1-bromohexane (10.7 g, 65 mmol), and elevated to room temperature and stirred for 12 h. The reaction was quenched with water and product was extracted with diethyl ether. The organic layer was washed with water, brine, and dried over MgSO₄, and then evaporated under reduced pressure. The residue was purified by flash column chromatography on silica gel with hexane as eluent to give **2a** as colorless liquid. Yield: 8.3 g (82%); IR (KBr): 3071 cm⁻¹ (sp² C–H),



Scheme 2. Synthesis of **HBTEA (13a)** and **DBTEA (13b)**. Reagents and conditions. (i) *n*-BuLi, 1-bromohexane; (ii) NBS, AcOH, chloroform; (iii) 2-methyl-3-butyn-2-ol, Pd(pph₃)₂Cl₂, Cul, Et₃N, reflux; (iv) KOH, *i*-PrOH, reflux; (v) Pd (dppf)₂Cl₂, Cul, toluene, *i*-Pr₂NH.

2921–2854 cm⁻¹ (sp³ C–H), 1470 cm⁻¹ (C=C); ¹H NMR (300 MHz, CDCl₃, ppm): δ 7.08 (d, 1H, *J*=4.8 Hz), 6.88 (dd, 1H, *J*=4.8 Hz), 6.69 (d, 1H, *J*=3.3 Hz), 2.81 (t, 2H, *J*=7.7 Hz), 1.68–1.61 (m, 2H), 1.34–1.26 (m, 6H), 1.02–0.98 (t, 3H, *J*=1.8 Hz); EIMS *m/z* (%): 168 (100, M⁺).

4.2.2. 2-Dodecylthiophene (2b). Compound **2b** was synthesized by the same procedure for synthesis of **2a**. Colorless liquid. Yield: 81%; IR (KBr): 3106–3038 cm⁻¹ (sp² C–H), 2923–2856 cm⁻¹ (sp³ C–H), 1475 cm⁻¹ (C=C); ¹H NMR (300 MHz, CDCl₃, ppm): δ 7.20–7.18 (dd, 1H, *J*=1.2 Hz), 7.03–7.00 (dd, 1H, *J*=3.3 Hz), 6.89–6.88 (dd, 1H, *J*=0.9 Hz), 2.96–2.91 (t, 2H, *J*=7.3 Hz), 1.85–1.75 (m, 2H), 1.41 (m, 18H), 1.05–1.00 (t, 3H, *J*=6.6 Hz); ¹³C NMR (75 MHz, CDCl₃, ppm): δ 145.85, 126.65, 122.74, 32.10, 30.06, 29.83, 29.55, 22.86, 14.25 Hz; EIMS *m/z* (%): 252 (100, M⁺).

4.2.3. 2-Bromo-5-hexylthiophene (3a). Compound **2a** (30 g, 178 mmol) was dissolved in chloroform/acetic acid (100 mL/100 mL, v/v) and added NBS (34.9 g, 198 mmol) at room temperature. The reaction mixture was stirred for 2 h and quenched with water (100 mL). The product was extracted with CH₂Cl₂ and washed with water, brine, and dried over MgSO₄, and then evaporated under reduced pressure. The residue was purified by flash column chromatography on silica gel with hexane as eluent to give **3a** as colorless liquid. Yield: 39 g (90%); IR (KBr): 3068 cm⁻¹ (sp² C–H), 2951–2852 cm⁻¹ (sp³ C–H), 1521–1436 cm⁻¹ (C=C); ¹H NMR (300 MHz, CDCl₃, ppm): δ 6.86–6.85 (d, 1H, *J*=3.6 Hz), 6.55–6.54 (d, 1H, *J*=3.6 Hz), 2.78–2.73 (t, 2H, *J*=7.2 Hz), 1.67–1.62 (m, 2H), 1.35–1.32 (m, 6H), 1.12–0.91 (t, 3H, *J*=1.8 Hz); ¹³C NMR (75 MHz, CDCl₃, ppm): δ 147.66, 129.37, 124.33, 108.55, 31.53, 31.43, 30.34, 28.66, 22.57, 14.08 Hz; EIMS *m/z* (%): 246 (100, M⁺).

4.2.4. 2-Bromo-5-dodecylthiophene (3b). Compound **3b** was synthesized by the same procedure for synthesis of **3a**. Colorless liquid.

Yield: 98%; IR (KBr): 3065 cm⁻¹ (sp² C–H), 2956–2858 cm⁻¹ (sp³ C–H), 1525–1433 cm⁻¹ (C=C); ¹H NMR (300 MHz, CDCl₃, ppm): δ 6.87–6.86 (d, 1H, *J*=3.6 Hz), 6.56–6.55 (d, 1H, *J*=3.6 Hz), 2.80–2.75 (t, 2H, *J*=7.6 Hz), 1.72–1.62 (m, 2H), 1.35–1.31 (m, 18H), 0.95–0.91 (t, 3H, *J*=6.6 Hz); ¹³C NMR (75 MHz, CDCl₃, ppm): δ 147.63, 129.36, 124.32, 108.59, 31.99, 31.51, 29.70, 29.60, 22.76, 14.18 Hz; EIMS *m/z* (%): 330 (100, M⁺).

4.2.5. [(5-Hexylthiophen-2-yl)ethynyl]trimethylsilane (4a). To a deaerated solution of **3a** (34.6 g, 140 mmol) in *i*-Pr₂NH (300 mL) were added Pd(pph₃)₂Cl₂ (2.25 g, 0.28 mmol) and Cul (1.6 g, 8.4 mmol) at room temperature. And then ethynyltrimethylsilane (19.4 mL, 140 mmol) was added dropwise to the reaction mixture and stirred at 90 °C for 12 h, and then allowed to reach at room temperature. The reaction mixture was filtered and solvent was removed by evaporation under reduced pressure and the residue performed flash column chromatography on silica gel with hexane as eluent to give **4a** as light brown liquid. Yield: 21.0 g (58%); IR (KBr): 2958–2927 cm⁻¹ (sp² C–H), 2853 cm⁻¹ (sp³ C–H), 2098 cm⁻¹ (C≡C), 1504–1465 cm⁻¹ (C=C); ¹H NMR (300 MHz, CDCl₃, ppm): δ 7.01–6.99 (d, 1H, *J*=3.3 Hz), 6.64–6.62 (d, 1H, *J*=3.6 Hz), 2.77–2.72 (t, 2H, *J*=7.2 Hz), 1.67–1.62 (m, 2H), 1.34–1.31 (m, 6H), 1.13–0.92 (t, 3H, *J*=1.8 Hz); ¹³C NMR (75 MHz, CDCl₃, ppm): δ 147.94, 131.94, 123.95, 119.93, 96.77, 75.98, 65.71, 31.95, 31.57, 31.36, 29.67, 29.39, 22.72, 14.15 Hz; EIMS *m/z* (%): 264 (100, M⁺).

4.2.6. 4-(5-Dodecylthiophen-2-yl)-2-methylbut-3-yn-2-ol (4b). To a deaerated solution of **3b** (3.93 g, 12 mmol) in Et₃N (40 mL) were added Pd(pph₃)₂Cl₂ (60 mg, 0.072 mmol) and Cul (8 mg, 0.04 mmol) at room temperature. And then 2-methyl-3-butyn-2-ol (1.172 mL, 18 mmol) was added to reaction mixture and stirred at 90 °C for 12 h, and then allowed to reach at room temperature. The reaction mixture was filtered and the solvent was removed under reduced

pressure and the residue performed flash column chromatography on silica gel with hexane/EtOAc (4:1, v/v) as eluent to give **4b** as light brown liquid. Yield: 2.97 g (73%); IR (KBr): 3652 cm^{-1} (O–H), 3071 cm^{-1} (sp^2 C–H), 2952–2844 cm^{-1} (sp^3 C–H), 2094 cm^{-1} ($\text{C}\equiv\text{C}$), 1498 cm^{-1} (C=C); ^1H NMR (300 MHz, CDCl_3 , ppm): δ 7.00–6.99 (d, 1H, $J=3.3$ Hz), 6.62–6.61 (d, 1H, $J=3.6$ Hz), 2.78–2.73 (t, 2H, $J=7.5$ Hz), 2.64 (s, 1H), 1.61 (m, 6H), 1.28 (m, 20H), 0.93–1.88 (t, 3H, $J=6.6$ Hz); ^{13}C NMR (75 MHz, CDCl_3 , ppm): δ 147.94, 131.94, 123.95, 119.93, 96.77, 75.98, 65.71, 31.95, 31.57, 31.36, 29.67, 29.39, 22.72, 14.15 Hz; HRMS: calcd for $\text{C}_{21}\text{H}_{34}\text{OS}$: 334.2330, found: 334.2331.

4.2.7. 2-Ethynyl-5-hexylthiophene (5a). To a solution of **4a** (21.35 g, 81 mmol) in THF (200 mL) was added Bu_4NF (1.0 M hexane, 28 mL, 28 mmol) at room temperature. The reaction mixture was stirred for 12 h. The reaction mixture was filtered, and the solvent was removed under reduced pressure and the residue performed flash column chromatography on silica gel with hexane as eluent to give **5a** as colorless oil. Yield: 10.0 g (64%); IR (KBr): 3288 cm^{-1} (sp C–H), 3065 cm^{-1} (sp^2 C–H), 2953–2856 cm^{-1} (sp^3 C–H), 2095 cm^{-1} ($\text{C}\equiv\text{C}$), 1523–1435 cm^{-1} (C=C); ^1H NMR (300 MHz, CDCl_3 , ppm): δ 7.13–7.12 (d, 1H, $J=3.6$ Hz), 6.67–6.66 (d, 1H, $J=3.6$ Hz), 3.31 (s, 1H), 2.83–2.80 (t, 2H, $J=7.6$ Hz), 1.71–1.64 (m, 2H), 1.36–1.33 (m, 6H), 0.96–0.91 (t, 3H, $J=6.7$ Hz); ^{13}C NMR (75 MHz, CDCl_3 , ppm): δ 148.56, 133.09, 123.97, 119.26, 80.42, 31.56, 31.54, 30.17, 28.75, 22.61; EIMS m/z (%): 192 (100, M^+).

4.2.8. 2-Dodecyl-5-ethynylthiophene (5b). To a solution of KOH (1.49 g, 27 mmol) and isopropyl alcohol (10 mL), **4b** (2.97 g, 9 mmol) in isopropyl alcohol (20 mL) was added dropwise with stirring for 30 min at 50 °C. And then the temperature of the reaction mixture increased to 80 °C and stirred for 12 h. After the completion of reaction, water was added for quenching, and extracted with ether. The solvent was removed under reduced pressure and the residue performed flash column chromatography on silica gel with *n*-hexane/EtOAc (4:1, v/v) as eluent to give **5b** as light brown color liquid. Yield: 1.63 g (65%); IR (KBr): 3283 cm^{-1} (sp C–H), 3063 cm^{-1} (sp^2 C–H), 2951–2858 cm^{-1} (sp^3 C–H), 2093 cm^{-1} ($\text{C}\equiv\text{C}$), 1523–1438 cm^{-1} (C=C); ^1H NMR (300 MHz, CDCl_3 , ppm): δ 7.12–7.10 (d, 1H, $J=3.6$ Hz), 6.65–6.64 (d, 1H, $J=3.6$ Hz), 3.30 (s, 1H), 2.81–2.76 (t, 2H, $J=7.5$ Hz), 1.69–1.65 (m, 2H), 1.33–1.28 (m, 18H), 0.93–0.88 (t, 3H, $J=6.7$ Hz); ^{13}C NMR (75 MHz, CDCl_3 , ppm): δ 148.60, 133.10, 123.95, 119.19, 80.38, 31.95, 31.56, 31.38, 30.15, 29.66, 29.56, 29.38, 29.04, 22.72, 14.15 Hz; EIMS m/z (%): 276 (100, M^+).

4.2.9. 2-(Anthracen-2-ylethynyl)-5-hexylthiophene (7a). To a solution of **6** (2.0 g, 7 mmol) in toluene and *i*- Pr_2NH (15 mL) were added Pd(dppf) $_2\text{Cl}_2$ (0.3 g, 0.37 mmol) and CuI (0.14 g, 0.73 mmol) at room temperature. And then **5a** (1.54 g, 67.3 mmol) in toluene (15 mL) and *i*- Pr_2NH (15 mL) were added dropwise to the reaction mixture. The reaction mixture was stirred for 12 h at 90 °C and then allowed to reach at room temperature. The reaction mixture was filtered and the solvent was removed under reduced pressure and the residue performed flash column chromatography on silica gel with hexane as eluent to give **7a** as yellow solid. Yield: 1.28 g (48%); mp: 128 °C; IR (KBr): 2956 cm^{-1} (sp^2 C–H), 2848 cm^{-1} (sp^3 C–H), 2096 cm^{-1} ($\text{C}\equiv\text{C}$), 1465 cm^{-1} (C=C); ^1H NMR (300 MHz, CDCl_3 , ppm): δ 8.40 (s, 2H), 8.20 (s, 1H), 8.03–7.96 (m, 3H), 7.51–7.48 (m, 3H), 7.19–7.18 (d, 1H, $J=3.6$ Hz), 6.73–6.72 (d, 1H, $J=3.6$ Hz), 2.86–2.81 (t, 2H, $J=7.5$ Hz), 1.76–1.66 (m, 2H), 1.38–1.34 (m, 6H), 0.95–0.90 (t, 3H, $J=6.7$ Hz); EIMS m/z (%): 368 (100, M^+). Anal. Calcd for $\text{C}_{26}\text{H}_{24}\text{S}$: C, 84.74; H, 6.56; S, 8.70. Found: C, 84.71; H, 6.47, S, 8.76.

4.2.10. 2-(Anthracen-2-ylethynyl)-5-dodecylthiophene (7b). Compound **7b** was synthesized by the same procedure for

synthesis of **7a**. Yellow colored solid. Yield: 47%; mp: 105 °C; IR (KBr): 2953–2918 cm^{-1} (sp^2 C–H), 2847 cm^{-1} (sp^3 C–H), 2102 cm^{-1} ($\text{C}\equiv\text{C}$), 1495 cm^{-1} (C=C); ^1H NMR (300 MHz, CDCl_3 , ppm): δ 8.40 (s, 2H), 8.20 (s, 1H), 8.04–7.96 (m, 3H), 7.53–7.48 (m, 3H), 7.18–7.17 (d, 1H, $J=3.6$ Hz), 6.73–6.72 (d, 1H, $J=3.6$ Hz), 2.86–2.81 (t, 2H, $J=7.6$ Hz), 1.76–1.66 (m, 2H), 1.28 (m, 18H), 0.92–0.88 (t, 3H, $J=6.6$ Hz); EIMS m/z (%): 452 (100, M^+). Anal. Calcd for $\text{C}_{32}\text{H}_{36}\text{S}$: C, 84.90; H, 8.02; S, 7.08. Found: C, 84.62; H, 8.09, S, 7.10.

4.2.11. 5-Hexyl-2,2'-bithiophene (9a). Compound **9a** was synthesized by the same procedure for synthesis of **2a**. Light green colored liquid. Yield: 75%; IR (KBr): 3078 cm^{-1} (sp^2 C–H), 2953–2853 cm^{-1} (sp^3 C–H), 1475–1428 cm^{-1} (C=C); ^1H NMR (300 MHz, CDCl_3 , ppm): δ 7.24–7.19 (m, 2H), 7.09–6.78 (m, 2H), 6.77–6.76 (d, 1H, $J=2.7$ Hz), 2.91–2.86 (t, 2H, $J=7.3$ Hz), 1.81–1.74 (m, 2H), 1.49–1.41 (m, 6H), 1.05–1.00 (t, 3H, $J=6.7$ Hz); ^{13}C NMR (75 MHz, CDCl_3 , ppm): δ 145.39, 138.10, 134.89, 127.76, 124.80, 123.75, 123.46, 123.04, 31.74, 30.28, 28.93, 22.76, 14.26 Hz; EIMS m/z (%): 250 (100, M^+).

4.2.12. 5-Dodecyl-2,2'-bithiophene (9b). Compound **9b** was synthesized by the same procedure for synthesis of **2a**. Light green colored liquid. Yield: 78%; IR (KBr): 3081 cm^{-1} (sp^2 C–H), 2956–2851 cm^{-1} (sp^3 C–H), 1478–1431 cm^{-1} (C=C); ^1H NMR (300 MHz, CDCl_3 , ppm): δ 7.23–7.19 (m, 2H), 7.09–7.05 (m, 2H), 6.77–6.76 (d, 1H, $J=3$ Hz), 2.90–2.85 (t, 2H, $J=7.5$ Hz), 1.83–1.74 (m, 2H), 1.39 (m, 18H), 1.04–1.00 (t, 3H, $J=6.6$ Hz); ^{13}C NMR (75 MHz, CDCl_3 , ppm): δ 145.34, 138.10, 134.89, 127.73, 124.77, 123.70, 123.41, 122.99, 32.13, 31.78, 29.86, 29.58, 22.90, 14.32 Hz; EIMS m/z (%): 334 (100, M^+).

4.2.13. 5-Bromo-5'-hexyl-2,2'-bithiophene (10a). Compound **10a** was synthesized by the same procedure for synthesis of **3a**. Light green colored liquid. Yield: 93%; IR (KBr): 3067 cm^{-1} (sp^2 C–H), 2955–2848 cm^{-1} (sp^3 C–H), 1515–1424 cm^{-1} (C=C); ^1H NMR (300 MHz, CDCl_3 , ppm): δ 6.97–6.94 (m, 2H), 6.86–6.85 (d, 1H, $J=3.6$ Hz), 6.70–6.69 (d, 1H, $J=3.3$ Hz), 2.84–2.79 (t, 2H, $J=7.6$ Hz), 1.73–1.66 (m, 2H), 1.41–1.35 (m, 6H), 0.95–0.92 (t, 3H, $J=3.4$ Hz); ^{13}C NMR (75 MHz, CDCl_3 , ppm): δ 145.93, 139.53, 133.76, 130.50, 124.81, 123.70, 123.01, 110.15, 31.60, 30.20, 28.83, 22.65, 14.17 Hz; EIMS m/z (%): 328 (100, M^+).

4.2.14. 5-Bromo-5'-dodecyl-2,2'-bithiophene (10b). Compound **10b** was synthesized by the same procedure for synthesis of **3a**. Light green colored liquid. Yield: 93%; IR (KBr): 3069 cm^{-1} (sp^2 C–H), 2953–2844 cm^{-1} (sp^3 C–H), 1518–1421 cm^{-1} (C=C); ^1H NMR (300 MHz, CDCl_3 , ppm): δ 6.98–6.95 (t, 2H, $J=4.0$ Hz), 6.87–6.86 (d, 1H, $J=3.9$ Hz), 6.71–6.70 (d, 1H, $J=3.6$ Hz), 2.85–2.80 (t, 2H, $J=7.6$ Hz), 1.78–1.68 (m, 2H), 1.39–1.34 (m, 18H), 0.99–0.95 (t, 3H, $J=6.6$ Hz); ^{13}C NMR (75 MHz, CDCl_3 , ppm): δ 145.88, 139.58, 133.82, 130.50, 124.82, 123.67, 122.96, 110.17, 32.09, 31.70, 30.26, 29.85, 29.82, 29.73, 29.54, 29.53, 29.25, 22.86, 14.30 Hz; EIMS m/z (%): 413 (100, M^+).

4.2.15. 4-(5'-Hexyl-2,2'-bithiophen-5-yl)-2-methylbut-3-yn-2-ol (11a). Compound **11a** was synthesized by the same procedure for synthesis of **4b**. Light brown colored solid. Yield: 82%; mp: 165 °C; IR (KBr): 3654 cm^{-1} (O–H), 3075 cm^{-1} (sp^2 C–H), 2951–2842 cm^{-1} (sp^3 C–H), 2098 cm^{-1} ($\text{C}\equiv\text{C}$), 1496 cm^{-1} (C=C); ^1H NMR (300 MHz, CDCl_3 , ppm): δ 7.07–7.06 (d, 1H, $J=3.6$ Hz), 6.99–6.98 (d, 1H, $J=3.3$ Hz), 6.95–6.93 (d, 1H, $J=3.9$ Hz), 6.69–6.68 (d, 1H, $J=3.6$ Hz), 2.82–2.77 (t, 2H, $J=7.5$ Hz), 2.19 (s, 1H), 1.71–1.66 (m, 2H), 1.63 (s, 6H), 1.37–1.32 (m, 6H), 0.93–0.89 (t, 3H, $J=6.7$ Hz); ^{13}C NMR (75 MHz, CDCl_3 , ppm): δ 146.18, 139.37, 134.03, 132.84, 124.88, 123.90, 122.51, 120.48, 98.14, 65.85, 31.56, 31.33, 30.18,

28.75, 22.58, 14.10 Hz; HRMS: calcd for $C_{19}H_{24}OS_2$: 332.1269, found: 332.1267.

4.2.16. 4-(5'-Dodecyl-2,2'-bithiophen-5-yl)-2-methylbut-3-yn-2-ol (11b). Compound **11b** was synthesized by the same procedure for synthesis of **4b**. Light brown colored solid. Yield: 73%; mp: 189 °C; IR (KBr): 3652 cm^{-1} (O–H), 3079 cm^{-1} (sp^2 C–H), 2956–2848 cm^{-1} (sp^3 C–H), 2094 cm^{-1} (C≡C), 1496 cm^{-1} (C=C); 1H NMR (300 MHz, $CDCl_3$, ppm): δ 7.07–7.06 (d, 1H, $J=3.6$ Hz), 6.99–6.98 (d, 1H, $J=3.6$ Hz), 6.95–6.93 (d, 1H, $J=3.6$ Hz), 6.69–6.68 (d, 1H, $J=3.6$ Hz), 2.82–2.77 (t, 2H, $J=7.5$ Hz), 2.09 (s, 1H), 1.73–1.63 (m, 6H), 1.40–1.28 (m, 18H), 0.92–0.88 (t, 3H, $J=6.6$ Hz); ^{13}C NMR (75 MHz, $CDCl_3$, ppm): δ 146.20, 139.38, 134.02, 132.85, 124.89, 123.90, 122.51, 120.44, 98.09, 65.84, 31.95, 31.33, 29.66, 29.57, 29.38, 22.72, 14.17; HRMS: calcd for $C_{25}H_{36}OS_2$: 416.2208, found: 416.2205.

4.2.17. 5-Ethynyl-5'-hexyl-2,2'-bithiophene (12a). Compound **12a** was synthesized by the same procedure for synthesis of **5b**. Brown colored liquid. Yield: 84%; IR (KBr): 3281 cm^{-1} (sp C–H), 3065 cm^{-1} (sp^2 C–H), 2948–2860 cm^{-1} (sp^3 C–H), 2091 cm^{-1} (C≡C), 1525–1441 cm^{-1} (C=C); 1H NMR (300 MHz, $CDCl_3$, ppm): δ 7.18–7.17 (d, 1H, $J=3.6$ Hz), 7.02–7.01 (d, 1H, $J=3.6$ Hz), 6.97–6.95 (d, 1H, $J=3.96$ Hz), 6.71–6.70 (d, 1H, $J=3.6$ Hz), 3.41 (s, 1H), 2.84–2.79 (t, 2H, $J=7.5$ Hz), 1.75–1.65 (m, 2H), 1.41–1.30 (m, 6H), 0.96–0.91 (t, 3H, $J=6.6$ Hz); ^{13}C NMR (75 MHz, $CDCl_3$, ppm): δ 146.40, 139.88, 133.91, 133.86, 124.93, 124.14, 122.42, 119.81, 81.95, 31.59, 30.21, 28.79, 22.62, 14.13 Hz; EIMS m/z (%): 274 (100, M^+).

4.2.18. 5-Dodecyl-5'-ethynyl-2,2'-bithiophene (12b). Compound **12b** was synthesized by the same procedure for synthesis of **5b**. Brown colored liquid. Yield: 66%; IR (KBr): 3286 cm^{-1} (sp C–H), 3069 cm^{-1} (sp^2 C–H), 2954–2847 cm^{-1} (sp^3 C–H), 2096 cm^{-1} (C≡C), 1496 cm^{-1} (C=C), 789 cm^{-1} (sp^2 C–H); 1H NMR (300 MHz, $CDCl_3$, ppm): δ 7.17–7.16 (d, 1H, $J=3.8$ Hz), 7.01–7.00 (d, 1H, $J=3.6$ Hz), 6.96–6.94 (d, 1H, $J=3.8$ Hz), 6.70–6.69 (d, 1H, $J=3.6$ Hz), 3.40 (s, 1H), 2.82–2.77 (t, 2H, $J=7.5$ Hz), 1.71–1.54 (m, 2H), 1.34–1.27 (m, 18H), 0.92–0.87 (t, 3H, $J=7.5$ Hz); ^{13}C NMR (75 MHz, $CDCl_3$, ppm): δ 146.4, 139.8, 133.9, 133.8, 124.9, 124.1, 122.4, 119.7, 82.9, 81.9, 31.9, 31.6, 30.1, 29.6, 29.5, 29.3, 29.0, 22.7, 14.1 Hz; HRMS: calcd for $C_{22}H_{30}S_2$: 358.1789, found: 358.1786.

4.2.19. 5-(Anthracen-2-ylethynyl)-5'-hexyl-2,2'-bithiophene (13a). Compound **13a** was synthesized by the same procedure for synthesis of **7a**. Yellow colored solid. Yield: 52%; mp: 195 °C; IR (KBr): 2919–2953 cm^{-1} (sp^2 C–H), 2850 cm^{-1} (sp^3 C–H), 2098 cm^{-1} (C≡C), 1604–1517 cm^{-1} (C=C); 1H NMR (300 MHz, $CDCl_3$, ppm): δ 8.41 (s, 2H), 8.22 (s, 1H), 8.03–7.97 (m, 3H), 7.52–7.49 (m, 3H), 7.24–7.23 (d, 1H, $J=3.6$ Hz), 7.05–7.03 (dd, 2H, $J=3.6$ Hz, $J=3.9$ Hz), 6.72–6.71 (d, 1H, $J=3.6$ Hz), 2.85–2.80 (t, 2H, $J=7.6$ Hz), 1.73–1.66 (m, 2H), 1.36–1.27 (m, 6H), 0.92–0.90 (t, 3H, $J=3.1$ Hz); EIMS m/z (%): 450 (100, M^+). Anal. Calcd for $C_{30}H_{26}S_2$: C, 79.95; H, 5.82; S, 14.23. Found: C, 79.79; H, 5.73, S, 14.24.

4.2.20. 5-(Anthracen-2-ylethynyl)-5'-dodecyl-2,2'-bithiophene (13b). Compound **13b** was synthesized by the same procedure for synthesis of **7a**. Light brown colored solid. Yield: 45%; mp: 191 °C; IR (KBr): 2928–2959 cm^{-1} (sp^2 C–H), 2864 cm^{-1} (sp^3 C–H), 2095 cm^{-1} (C≡C), 1495 cm^{-1} (C=C); 1H NMR (300 MHz,

$CDCl_3$, ppm): δ 8.41 (s, 2H), 8.22 (s, 1H), 8.04–7.97 (m, 3H), 7.53–7.49 (m, 3H), 7.24–7.23 (d, 1H, $J=3.9$ Hz), 7.05–7.02 (dd, 2H, $J=3.6$, 3.9 Hz), 6.72–6.71 (d, 1H, $J=3.6$ Hz), 2.85–2.79 (t, 2H, $J=7.6$ Hz), 1.75–1.65 (m, 2H), 1.28 (m, 18H), 0.92–0.87 (t, 3H, $J=6.7$ Hz); EIMS m/z (%): 534 (100, M^+). Anal. Calcd for $C_{36}H_{38}S_2$: C, 80.85; H, 7.16; S, 11.99. Found: C, 80.81; H, 7.11, S, 11.92.

Acknowledgements

This research was supported by the Basic Science Research Program through the National Research Foundation of Korea (NRF) funded by the Ministry of Education, Science and Technology (Grant Number: 2010-0023775).

Supplementary data

HRMS and elemental analysis data are included. Supplementary data associated with this article can be found in the online version, at <http://dx.doi.org/10.1016/j.tet.2013.07.041>.

References and notes

- Lim, E.; Jung, B.-J.; Shim, H.-K. *J. Polym. Sci., Part A: Polym. Chem.* **2005**, *44*, 243.
- Lee, J.; Cho, H. J.; Cho, N. S.; Hwang, D.-H.; Kang, J.-M.; Lim, E.; Lee, J.-L.; Shim, H.-K. *J. Polym. Sci., Part A: Polym. Chem.* **2006**, *44*, 2943.
- Yang, R.; Tian, R.; Hou, Q.; Zhang, Y.; Li, Y.; Yang, W.; Zhang, C.; Cao, Y. *J. Polym. Sci., Part A: Polym. Chem.* **2005**, *43*, 823.
- Katz, H. E.; Bao, Z.; Gilat, S. L. *Acc. Chem. Res.* **2001**, *34*, 359.
- Horowitz, G. *Adv. Mater.* **1998**, *10*, 365.
- Brabec, C. J.; Sariciftci, N. S.; Hummelen, J. C. *Adv. Funct. Mater.* **2001**, *11*, 15.
- Lee, J.; Jung, B. J.; Lee, S. K.; Lee, J. I.; Cho, H. J.; Shim, H. K. *J. Polym. Sci., Part A: Polym. Chem.* **2005**, *43*, 1845.
- Linrun, F.; Xiaoli, X.; Xiaojun, G. *ECS Trans.* **2011**, *37*, 105.
- Fujisaki, Y.; Nakajima, Y.; Takei, T.; Fukagawa, H. *IEEE Trans. Electron Devices* **2012**, *59*, 3442.
- Orgiu, E.; Masillamani, A.; Vogel, J.-O.; Treossi, E.; Kiersnowski, A.; Kastler, M.; Pisula, W.; Doetz, F.; Palermo, V.; Samori, P. *Chem. Commun.* **2012**, 1562.
- Youn, J.; Huang, P.; Huang, Y.; Chen, M.; Lin, Y.-J.; Huang, H.; Ortiz, R. P.; Stern, C.; Chung, M.-C.; Feng, C.-Y. *Adv. Funct. Mater.* **2012**, *22*, 48.
- Sunhee, P.; Jaemin, L.; Jung, M. K.; Hyun, S. L.; Jongsun, L.; Seung, H. C.; Jun, Y. L.; Changjin, L. *Mol. Cryst. Liq. Cryst.* **2009**, *504*, 52.
- Ong, B. S.; Wu, Y.; Li, Y.; Liu, P.; Pan, H. *Chem.—Eur. J.* **2008**, *14*, 4766.
- Kong, H.; Chung, D. S.; Kang, I.-N.; Lim, E.; Jung, Y. K.; Park, J.-H.; Park, C. E.; Shim, H.-K. *Bull. Korean Chem. Soc.* **2007**, *28*, 1945.
- Inoue, Y.; Tokito, S.; Ito, K.; Suzuki, T. *J. Appl. Phys.* **2004**, *95*, 5795.
- Meng, H.; Sun, F.; Goldfinger, M. B.; Gao, F.; Londono, D. J.; Marshal, W. J.; Blackman, G. S.; Dobbs, K. D.; Keys, D. E. *J. Am. Chem. Soc.* **2006**, *128*, 9304.
- He, Z.; Xiao, K.; Durant, W.; Hensley, D. K.; Anthony, J. E.; Hong, K.; Kilbey, S. M.; Chen, J.; Li, D. *Adv. Funct. Mater.* **2011**, *21*, 3617.
- Yuan, G.-C.; Lu, Z.; Xu, Z.; Gong, C.; Qun-Liang Song, Q.-L.; Zhao, S.-L.; Zhang, F.-J.; Xua, N.; Gan, Y.; Yang, H.-B.; Li, C.-M. *Org. Electron.* **2009**, *10*, 1388.
- Kwon, J.; Hong, J.-P.; Lee, W.; Noh, S.; Lee, C.; Lee, S.; Hong, J.-I. *Org. Electron.* **2010**, *11*, 1103.
- Tszydel, I.; Kucinska, M.; Marszalek, T.; Rybakiewicz, R.; Nosal, A.; Jung, J.; Gazicki-Lipman, M.; Pitsalidis, C.; Gravalidis, C. *Adv. Funct. Mater.* **2012**, *22*, 3840.
- Kim, S.-O.; An, T. K.; Chen, J.; Kang, I. I.; Kang, S. H.; Chung, D. S.; Park, C. E.; Kim, Y.-H.; Kwon, S.-K. *Adv. Funct. Mater.* **2011**, *21*, 1616.
- Hwang, M. J.; Park, J. H.; Jeong, E. B.; Kang, I. L.; Lee, D. H.; Park, C. E.; Singh, O. M.; Choi, H. J.; Kim, Y.-H.; Yoon, Y. J. *Bull. Korean Chem. Soc.* **2012**, *33*, 3810.
- Menzel, H.; Weichart, B.; Schmidt, A.; Paul, S.; Knoll, W.; Stumpe, J.; Fischer, T. *Langmuir* **1994**, *10*, 1926.
- (a) Spano, F. C. *Annu. Rev. Phys. Chem.* **2006**, *57*, 217; (b) Meinardi, F.; Cerminara, M.; Sassella, A.; Bonifacio, R.; Tubino, R. *Phys. Rev. Lett.* **2003**, *91*, 247401.
- Spano, F. C. *Acc. Chem. Res.* **2010**, *43*, 429.
- Drolet, N.; Morin, J.-F.; Leclerc, N.; Wakim, S.; Tao, Y.; Leclerc, M. *Adv. Funct. Mater.* **2005**, *15*, 1671.
- Coleman, R. S.; Mortensen, M. A. *Tetrahedron Lett.* **2003**, *44*, 1215.
- Tao, X.-C.; Zhou, W.; Zhang, Y.-P.; Dai, C.-Y.; Shen, D.; Huang, M. *Chin. J. Chem.* **2006**, *24*, 939.